Detection of the tau protein in human serum by a sensitive four-electrode electrochemical biosensor

Scarlet Xiaoyan Wang[1], Desiree Acha[1], Ajit J Shah[1], Frank Hills[1], Ivan Roitt[1], Andreas Demosthenous[2], Richard H Bayford[1*]

[1] Department of Natural Sciences, Middlesex University, UK
[2] Department of Electronic and Electrical Engineering, University College London, UK.

[*]Corresponding author. Tel: +44(0)7771773140. Email: r.bayford@mdx.ac.uk

Abstract

This study presents a novel approach based on a four-electrode electrochemical biosensor for the detection of tau protein - one of the possible markers for the prediction of Alzheimer's disease (AD). The biosensor is based on the formation of stable antibody–antigen complexes on gold microband electrodes covered with a layer of a self-assembled monolayer and protein G. Antibodies were immobilized on the gold electrode surface in an optimal orientation by protein G interaction. Electrochemical impedance spectroscopy was used to analyze impedance change, which revealed a linear response with increasing tau concentrations. The assay is fast (<1 h for incubation and measurement) and very sensitive. The limit of quantification for the full-length 2N4R tau protein is 0.03 pM, a value unaltered when the assay was processed in bovine serum albumin or human serum. This technology could be adapted for the detection of other biomarkers to provide a multiple assay to identify AD progression in a point of care setting.

Keywords: Alzheimer's disease, biomarker, electrochemical biosensor, impedance, tau

1. Introduction

Alzheimer's disease (AD) is the most common form of dementia, with an estimated 37 million sufferers worldwide and is expected to affect 115 million by 2050 if no effective therapeutic strategies are developed (Wimo et al., 2013). The enormous worldwide costs of dementia are expected to rise in the next few years. AD is becoming more prevalent due to the ageing of society and the lack of effective drugs to improve or cure established disease. Currently, AD diagnosis is complex, costly and inaccurate. Procedures including neuropsychological tests, magnetic resonance imaging and clinical assessment are used to assist diagnosis but currently confirmation at autopsy is the only reliable way to diagnose AD.

AD is characterized by protein misfolding commencing years before substantial neurodegeneration. It can take over a decade to develop AD (Perrin et al., 2009; Price and Morris, 1999), making early diagnosis possible and crucial. There are six isoforms of tau protein expressed in the human brain (Goedert et al., 1989) which promote microtubule polymerization and stabilization in the nervous system (Caceres and Kosik, 1990; Drubin and Kirschner, 1986; Goedert et al., 1989; Horio and Hotani). Tau can undergo aberrant hyperphosphorylation at various sites and fail to stabilize the microtubules, contributing to neurofibrillary tangles and paired helical filaments formation (Hanger et al., 1998; Lu and Wood, 1993; Mandelkow and Mandelkow, 1998; von Linstow Roloff and Platt, 1999) which, alongside amyloid-beta (Aβ) plaques, are two prominent pathological hallmarks of AD (Brækhus, 2011; Kosik, 1991; Lee and Trojanowski, 1992). Historically, tau pathology was considered secondary to Aβ pathology. However, the accumulation of abnormal tau species is now

known to more accurately predict disease severity (Cook et al., 2015). Both cognitive decline rate and postmortem AD classification into pathological subtypes are determined by the tau pathology in the brain (Murray et al., 2011). Tau levels in cerebro-spinal fluid (CSF) increase slightly with ageing. Several studies demonstrated that CSF tau levels are significantly increased in AD patients (Brys et al., 2009; H Hampel et al., 2004; Harald Hampel et al., 2004; Hu et al., 2002; Mandelkow and Mandelkow, 1998; Mattsson et al., 2009; Shoji et al.), indicating tau as a critical biomarker for early AD diagnosis. Sunderland *et al* (2003) demonstrated that a cut-off value of 4.3 pM tau in CSF can differentiate AD cases with 92% sensitivity and 89% specificity (Sunderland et al.).

Tau CSF levels have been measured with conventional methods such as enzyme-linked immunosorbent assay (ELISA), mass spectrometry or surface plasmon resonance, which are time-consuming and/or expensive (Hye et al., 2014; Liu et al., 2014; Mehta et al., 2000; Sparks et al., 2012; Tuantranont, 2013). Researchers have made great efforts to generate rapid, cost-effective and highly sensitive detection tests using biosensors. For example, Rushworth *et al*. developed a label-free electrochemical biosensor which detects Aβ oligomers (Rushworth et al., 2014). Recently, an electrochemical biosensor was developed for tau, although the level of detection is 0.2 μM - about 5 orders of magnitude higher than the CSF tau cut-off value (4.3 pM) which distinguishes AD cases from control (Esteves-Villanueva et al., 2014).

In this study we have developed a novel, very sensitive electrochemical biosensor for detection of full-length 2N4R tau protein based on a microelectrode array with four gold microband electrodes[1] coated with oriented antibodies. The biosensor was specific for full-length tau detection with a limit of quantification of 0.03 pM - much lower than the critical cut-off value (4.3 pM) of CSF tau protein. We have also demonstrated the selectivity of this technique. The presence of bovine serum albumin (BSA) has been shown to interfere with detection of low-abundant biomarkers in biological fluid (Tuantranont, 2013). In this study, no significant interference from BSA or human serum (HS) was observed. Although tau is the focus of this study, there is still not a consensus on the range of markers associated with AD and this biosensor could be adapted to detect a range of such markers.

2. Materials and methods

2.1 Materials

The gold microband electrodes (AUMB4000-M) were manufactured by Windsor Scientific (UK). 3,3'-dithiobis(sulfosuccinimidyl propionate) (DTSSP), protein G, phosphate buffered saline (PBS), sulphuric acid and Dulbecco's modified eagle medium (DMEM) were purchased from Thermo Fisher Scientific (UK). Ethanolamine, BSA, skimmed milk powder, 3,3',5,5'-tetramethylbenzidine liquid substrate and Tween20 were obtained from Sigma-Aldrich (UK). Anti-tau antibody (39E10) and human full-length tau441 were from Cambridge Bioscience (UK). Polyvinylidene difluoride (PVDF) membrane was purchased from Millipore Corporation, Bedford, MA, USA. Horseradish peroxidase (HRP) conjugated anti-mouse antibody and HRP conjugated anti-His antibody were purchased from Abcam, UK. HS taken from confirmed normal individuals was purchased from BBI Solutions, UK.

2.2 Development of the biosensor

The biosensor was developed on a microelectrode array (from Windsor Scientific, UK) composed of four gold microband electrodes fabricated using standard microfabrication technology on a p-doped

[1] The tetrapolar technique (four electrodes) has the advantage that the electrode configuration can be adjusted to maximise the sensitivity of the impedance change in different biological and chemical layers. More importantly, unlike the three electrode method used in Sharma et al. 2016, the tetrapolar method improves the sensitivity of the voltage measurement obtained from the tau layer (Kassanos et al., 2008a).

silicon substrate (Fig. 1). The gold surface was coated with an organic polymer passivation layer, leaving an open window of 1 × 1 mm exposing a 1 mm length of each gold microband electrode - the active area.

The microelectrode array was connected to a printed circuit board via four gold-plated pins and then to the appropriate BNC socket of the impedance analyser. The first electrode was the working electrode (WE), to which the signal generator output of the impedance analyser was connected. The fourth electrode was the counter electrode (CE). This was connected to the instrument's current input BNC socket. The second and third electrodes were reference electrodes (RE) and were connected respectively to the instrument's V1 Hi and V1 Lo BNCs (Fig. 1). A shield was used to protect the measurements from external electromagnetic noise.

The gold microband electrodes were washed with 5 mL of 100% ethanol, de-ionized water and PBS to remove any dielectric material from the sensor surface. Cross-linker DTSSP was attached to the cleaned microband electrodes by dissociative chemisorbtion forming a self-assembled monolayer (SAM). Protein G and antibodies were added layer by layer, incubating each for 45 min in PBS, with washing steps in between. DTSSP attaches protein G via the interaction between the sulpho-NHS ester and amino groups. Ethanolamine was used to saturate unreacted sulpho-NHS ester group in DTSSP after protein G binding before addition of antibody. Different concentrations of anti-tau antibody were applied (see supporting information, Fig. S1). The optimal concentration of 125 µg/ml of anti-tau antibody was used throughout the following experiments.

2.3 Electrochemical impedance spectroscopy (EIS)

At each stage of biosensor assembly, impedance measurements were conducted in 10 mM $K_4Fe(CN)_6/K_3Fe(CN)_6$ (1:1 ratio) in PBS pH 7 using Smart software on a Solartron Impedance/Gain-Phase Analyser 1260 model (Solartron Analytical, UK). A sinusoidal signal of 5 mV amplitude was applied between electrodes WE and CE (Fig. 1) using a frequency range 40-40,000 Hz to produce EIS measurements. The fully built biosensor was subjected to successive incubations in tau or BSA (10^{-14} M, 10^{-12} M, 10^{-10} M, 10^{-8} M, and 10^{-7} M) for 25 min at room temperature. After each reaction, the biosensor electrodes were flood washed with 5 mL of de-ionized water and PBS before recording the impedance in 10 mM $K_4Fe(CN)_6/K_3Fe(CN)_6$ (1:1 ratio) in PBS pH 7 as described above. EIS parameters R_s (solution resistance), R_{ct} (charge-transfer resistance or interfacial resistance) and C_p (constant phase element, an equivalent model of double-layer capacitance) were generated by fitting the data to the Randles′ equivalent circuit model using Zview software (Solartron Analytical, UK).

2.3 Cyclic voltammetry

Cyclic voltammetry (CV) was performed in sulphuric acid for electrode regeneration and in 10 mM $K_4Fe(CN)_6/K_3Fe(CN)_6$ (1:1 ratio) in PBS pH 7 for the biosensor layer-by-layer construction. For electrode regeneration, the potential was cycled from -0.1 V to +1.74 V at 100 mV s^{-1} SCE (saturated calomel electrode) 4 or 5 times to remove surface analytes and/or contaminants. For biosensor construction, scans were conducted between -0.4 V and +0.8 V.

2.4 Tau detection by Western blotting

Following electrophoresis, proteins were transferred to an activated PVDF membrane. Transfer was carried out in a Trans-Blot Semi-Dry transfer machine (Bio-Rad Laboratories, Hercules, CA, USA) and run at 50 mA for 90 min. Membranes were incubated in 5% skimmed milk in PBS-0.1% Tween20 (PBST) at room temperature for 1 h prior to incubation in primary mouse anti-tau antibody (39E10) diluted 1:1000 with 1% milk in PBST for 1 h at room temperature. This was followed by three 15 min washes in PBST. HRP conjugated anti-mouse antibody was diluted 1:5000 with 1% milk

in PBST and incubated with membrane for 1 h at room temperature. Membranes were then washed three times as before. Proteins were visualised by chemiluminescence detection with ECL PLUS (Amersham Pharmacia Biotech, Piscataway, NJ, USA) for 5 min and analyzed using the LI-COR system (LI-COR Biosciences, USA).

2.5 ELISA

ELISA was carried out to determine the interaction between tau antibody (39E10) and tau. 1 µg/mL 39E10 was coated on 96-well Maxisorp plates (NUNC. Denmark) at 4 ºC overnight. After blocking with 200 µL/well Microwell Blocking Buffer with Stabilizer (Rockland), serial dilutions of tau in PBS or tau in 5% HS pH 7, were added to the plates for 1 h. After three washes with PBS, HRP conjugated anti-His antibody (1:2500 dilution) was added to detect the bound tau. 3,3',5,5'-tetramethylbenzidine liquid substrate was added and left to develop for 30 min at room temperature. The reaction was stopped with 2M sulphuric acid and absorbance measured at 450 nm.

3. Results

3.1. Confirmation of biosensor assembly by EIS and CV

The biosensor was constructed on four gold microband electrodes (Fig. 1). SAM was deposited as described in Section 2.2 after the gold electrodes were cleaned with ethanol, followed by incubation with protein G and antibodies for 45 min in PBS, with washing in between. We adapted the construction of our previous biosensor (Kassanos et al., 2008b) using a layer of protein G, to ensure that antibody Fab binding domains were oriented away from the biosensor surface and free to react with target antigens. This increases the loading capacity of the biosensor and its sensitivity to antigens. Additionally, it significantly improves reproducibility, since the antibodies do not attach randomly to the surface.

EIS is widely used to validate the layer-by-layer deposition of materials to a sensor surface because it is a very powerful tool for surface interface characterization and detection of changes to biosensor surfaces (Bryan et al., 2012; Rushworth et al., 2014). Here, impedance measurements were performed at each stage of the assembly in 10 mM $K_4Fe(CN)_6/K_3Fe(CN)_6$ (1:1 ratio) in PBS pH 7 over a frequency range 40-40,000 Hz. These spectra are typical of the theoretical, semi-circular shape when fitted to a Randles′ equivalent circuit (a useful tool in interpreting EIS data which accounts for the resistive and capacitive processes at different frequencies). An example of Nyquist plots of the measured EIS data from a sample biosensor is shown in Fig. 2A. Fitting the data to the Randles′ equivalent circuit model, demonstrated that the interfacial charge-transfer resistance (R_{ct}) changed after each layer was deposited (Fig. 2B), namely bare gold, DTSSP or SAM, protein G, ethanolamine and antibody. This indicates the successful construction of the biosensor. It is widely reported that analyte binding to biosensor surfaces often causes increased impedance, typically due to increasing deposition of a substance on the sensor surface which increases its surface capacitance and resistance (Martic et al., 2013). However, although less widely reported, the binding of certain analytes to electrochemical biosensors can decrease the surface impedance (Rushworth et al., 2014). The same reaction was observed here. The attachment of anti-tau to the functionalised surface may increase the conductivity of the surface and thus cause a decrease in impedance change (Fig. 2B). The construction of the biosensor and the assembly of each layer were also confirmed by CV (Fig. 2C).

3.2. Detection of tau by the biosensor

The biosensor was incubated with successive concentrations of tau (10^{-14} M to 10^{-7} M) for 25 min each, followed by flood washing with dH_2O and PBS. Impedance was recorded with the biosensor immersed in 10 mM $K_4Fe(CN)_6/K_3Fe(CN)_6$ (1:1 ratio) in PBS pH 7 over a frequency range of 40-40,000 Hz. The measured EIS data from a sample biosensor are presented as Nyquist plots in Fig. 3. Generated EIS parameters R_s (solution resistance), R_{ct} (charge-transfer resistance) and C_p (constant phase element, an equivalent model of double-layer capacitance) after fitting the data to the Randles′ equivalent circuit, are listed in Table 1. R_{ct} was the parameter used to evaluate analyte-biosensor binding in the experiments because it is based on Faradaic impedance, measured in the presence of redox mediators (Rushworth et al., 2014). R_{ct} values increased upon addition of increasing concentrations of tau (10^{-14} M to 10^{-7} M) as demonstrated by the increasing height and diameter of the semi-circular Nyquist traces (Fig. 3A), corresponding to increased capacitance and resistance of the sensor surface respectively. As reported before, the binding of analyte to a biosensor surface often causes an increase in impedance (Martic et al., 2013; Rains et al., 2013).

3.3. Calibration curves of tau binding to the biosensor

Biosensor specificity and selectivity were analysed by incubation with BSA - a commonly used plasma protein standard. Albumin is the most-abundant protein component in serum and CSF. Multiple biosensors ($n \geq 3$) were incubated in the presence of either tau or BSA (negative control) as described in Section 2.2. The R_{ct} values for each analyte concentration were calculated by fitting semi-circle spectra to the Randles′ equivalent circuit model. The R_{ct} values following incubation with increasing concentrations of tau and BSA are shown in Fig. 3B. There was a trend of increasing interfacial resistance after tau binding, while no significant response was detected following BSA incubation. The R_{ct} value for tau binding reached a plateau with no further increase at 10^{-8} M indicating saturation of the biosensor interfacial surface. The inset in Fig. 3B demonstrates the relationship between interfacial resistance change and tau concentrations (0.01 pM to 10 nM) constructed from R_{ct} values from at least three independent experiments. The biosensor response to tau was quantified as $(R_{ct} - R_{ct0})/R_{ct0}$, where R_{ct0} represents the R_{ct} value of biosensor with antibody deposition. The limit of detection (LOD) calculated according to IUPAC (International Union of Pure and Applied Chemistry) was 0.03 pM (Loo et al., 2014).

The selectivity and specificity of tau antibody was investigated by Western blotting (Fig. 3C inset). Different concentrations of tau in PBS or HS were transferred to PVDF membrane before incubation with anti-tau antibody and HRP conjugated anti-mouse antibody as described in Section 2.2. ECL reagent was used to generate a chemiluminescent signal. An increasing signal was detected for increasing tau concentrations, while no signal was detected with HS only (Fig. 3C inset), indicating the tau specificity. Specificity was further confirmed by incubating multiple biosensors ($n \geq 3$) with BSA. The biosensor was unresponsive to BSA incubation (10^{-14} M to 10^{-6} M, Fig. 3C). The percentage change of R_{ct} was < 4% at 10^{-6} M BSA, compared to > 60% at a tau concentration of 10^{-14} M.

3.4. Validation of the biosensor using human serum (HS) spiked with tau

Finally, we evaluated the ability of the biosensor to detect tau in HS. Serum spiked with different tau concentrations was incubated with the biosensor and EIS was conducted in 10 mM $K_4Fe(CN)_6/K_3Fe(CN)_6$ (1:1 ratio) pH 7 under standard conditions over a frequency range of 40-40,000 Hz as described in Section 2.2. The trend of biosensor response to tau in HS in Nyquist plots

(Fig. 4) was similar to that seen for tau only (Fig. 3), indicating that the biosensor specifically recognizes tau at 10^{-14} M in HS. Biosensor response was not affected following incubation with HS at a range of dilutions in PBS indicating that components of serum do not interfere with tau measurement (Fig. 4B). Although the % change of R_{ct} versus full biosensor (R_{ct0}) was lower than that for tau only, the relative increase (three fold) was similar between the tau concentration range of 10^{-14} and 10^{-8} M for tau in PBS (0.6-1.6) (Fig. 3B) and tau in a dilution of 1:1 in HS (0.08-0.29) (Fig. 4C), indicating that HS did not affect assay specificity or sensitivity. The low change of R_{ct} may be due to the small electrode size and non-specific interference of HS to the biosensor also seen in ELISA (Fig. 5A).

3.5. Comparison between electrochemical biosensor and ELISA

ELISA was carried out to determine the LOD of tau by anti-tau antibody. LOD was defined as the lowest concentration of tau that was distinguishable from HS in the absence of tau. ELISA took several hours while the electrochemical biosensor testing took less than 1 h for incubation and measurement. The LOD by the biosensor (10^{-14} M) was greatly superior to that for ELISA (10^{-8} M) as shown in Fig. 5.

4. Conclusions and future work

In this study, we extended the development of a novel electrochemical biosensor based on tetrapolar EIS, which allows adjustment of the sensitivity of detection of different layers of material binding to the electrode surface (Kassanos et al., 2008b). Our data indicate that the sensor can rapidly detect tau as low as 0.03 pM which is much lower than the detection limit of ELISA in this study (10 nM) and the commercial ELISA kit (Thermofisher Scientific, UK, 0.25 pM), both of which take at least 4 h to complete. The specificity of the bioreceptor for tau binding was confirmed by Western blotting. The results suggest that the biosensor could be used to quantify tau in CSF and serum.

We have validated this biosensor for measurement in both serum and PBS buffer. In a previous study examining AD biomarkers from CSF (Rushworth et al 2014), it was observed that serum and CSF are complex media but provide comparable results. We believe that this is a good indication that the biosensor in this study will perform equally well in CSF. Crucially, in our biosensor we have also demonstrated that albumin, the most abundant protein component of both serum and CSF, does not interfere with tau measurement. It would, of course, be of interest to compare the performance of this method in CSF.

Compared to previous biosensors for tau detection (Esteves-Villanueva et al., 2014), ours is extremely sensitive, highly specific and allows detection in HS down to 0.03 pM which is diagnostically important for AD. It was noted that there is a variation in the response of PBS to HS for the biosensor. It is likely that this is due to a variation of the ion concentration in the different media, which could be addressed by using different electrode spacing for different media. There is scope to further improve the biosensor characteristics by increasing the electrode surface area and using Fab fragments as bioreceptors. The utilization of protein G and antibodies of differing specificities would enable the development of a multiplex device where multiple biosensors functionalized with different bioreceptors could be employed for simultaneous detection of multiple AD biomarkers.

Acknowledgements

We would like to thank Dr. Lei Wang for his assistance in statistical analysis and Dr. Dai Jiang for his suggestions and design of the printed circuit board.

References

Brækhus, A., 2011. [Biomarkers of dementia]. Tidsskr. den Nor. lægeforening Tidsskr. Prakt. Med. ny række 131, 2218. doi:10.4061/2011/564321

Bryan, T., Luo, X., Forsgren, L., Morozova-Roche, L. a., Davis, J.J., 2012. The robust electrochemical detection of a Parkinson's disease marker in whole blood sera. Chem. Sci. 3, 3468. doi:10.1039/c2sc21221h

Brys, M., Pirraglia, E., Rich, K., Rolstad, S., Mosconi, L., Switalski, R., Glodzik-Sobanska, L., De Santi, S., Zinkowski, R., Mehta, P., Pratico, D., Saint Louis, L.A., Wallin, A., Blennow, K., de Leon, M.J., 2009. Prediction and longitudinal study of CSF biomarkers in mild cognitive impairment. Neurobiol. Aging 30, 682–90. doi:10.1016/j.neurobiolaging.2007.08.010

Caceres, A., Kosik, K.S., 1990. Inhibition of neurite polarity by tau antisense oligonucleotides in primary cerebellar neurons. Nature 343, 461–3. doi:10.1038/343461a0

Cook, C.N., Murray, M.E., Petrucelli, L., 2015. Understanding Biomarkers of Neurodegeneration: Novel approaches to detecting tau pathology. Nat. Med. 21, 219–220. doi:10.1038/nm.3809

Drubin, D.G., Kirschner, M.W., 1986. Tau protein function in living cells. J. Cell Biol. 103, 2739–46.

Esteves-Villanueva, J.O., Trzeciakiewicz, H., Martic, S., 2014. A protein-based electrochemical biosensor for detection of tau protein, a neurodegenerative disease biomarker. Analyst 139, 2823–31. doi:10.1039/c4an00204k

Goedert, M., Spillantini, M.G., Jakes, R., Rutherford, D., Crowther, R.A., 1989. Multiple isoforms of human microtubule-associated protein tau: sequences and localization in neurofibrillary tangles of Alzheimer's disease. Neuron 3, 519–26.

Hampel, H., Buerger, K., Zinkowski, R., Teipel, S.J., Goernitz, A., Andreasen, N., Sjoegren, M., DeBernardis, J., Kerkman, D., Ishiguro, K., Ohno, H., Vanmechelen, E., Vanderstichele, H., McCulloch, C., Moller, H.-J., Davies, P., Blennow, K., 2004. Measurement of phosphorylated tau epitopes in the differential diagnosis of Alzheimer disease: a comparative cerebrospinal fluid study. Arch. Gen. Psychiatry 61, 95–102. doi:10.1001/archpsyc.61.1.95

Hampel, H., Teipel, S.J., Fuchsberger, T., Andreasen, N., Wiltfang, J., Otto, M., Shen, Y., Dodel, R., Du, Y., Farlow, M., Möller, H.-J., Blennow, K., Buerger, K., 2004. Value of CSF beta-amyloid1-42 and tau as predictors of Alzheimer's disease in patients with mild cognitive impairment. Mol. Psychiatry 9, 705–10. doi:10.1038/sj.mp.4001473

Hanger, D.P., Betts, J.C., Loviny, T.L., Blackstock, W.P., Anderton, B.H., 1998. New phosphorylation sites identified in hyperphosphorylated tau (paired helical filament-tau) from Alzheimer's disease brain using nanoelectrospray mass spectrometry. J. Neurochem. 71, 2465–76.

Horio, T., Hotani, H.,. Visualization of the dynamic instability of individual microtubules by dark-field microscopy. Nature 321, 605–7. doi:10.1038/321605a0

Hu, Y.Y., He, S.S., Wang, X., Duan, Q.H., Grundke-Iqbal, I., Iqbal, K., Wang, J., 2002. Levels of nonphosphorylated and phosphorylated tau in cerebrospinal fluid of Alzheimer's disease patients : an ultrasensitive bienzyme-substrate-recycle enzyme-linked immunosorbent assay. Am. J. Pathol. 160, 1269–78. doi:10.1016/S0002-9440(10)62554-0

Hye, A., Riddoch-Contreras, J., Baird, A.L., Ashton, N.J., Bazenet, C., Leung, R., Westman, E., Simmons, A., Dobson, R., Sattlecker, M., Lupton, M., Lunnon, K., Keohane, A., Ward, M., Pike, I., Zucht, H.D., Pepin, D., Zheng, W., Tunnicliffe, A., Richardson, J., Gauthier, S., Soininen, H., Kłoszewska, I., Mecocci, P., Tsolaki, M., Vellas, B., Lovestone, S., 2014. Plasma proteins predict conversion to dementia from prodromal disease. Alzheimer's Dement. 44, 1–9. doi:10.1016/j.jalz.2014.05.1749

Kassanos, P., Demosthenous, A., Bayford, R.H., 2008a. Towards an optimized design for tetrapolar affinity-based impedimetric immunosensors for lab-on-a-chip applications, in: 2008 IEEE Biomedical Circuits and Systems Conference. IEEE, pp. 141–144. doi:10.1109/BIOCAS.2008.4696894

Kassanos, P., Iles, R.K., Bayford, R.H., Demosthenous, A., 2008b. Towards the development of an electrochemical biosensor for hCGbeta detection. Physiol. Meas. 29, S241–S254. doi:10.1088/0967-3334/29/6/S21

Kosik, K.S., 1991. Alzheimer plaques and tangles: advances on both fronts. Trends Neurosci. 14, 218–9.

Lee, V.M., Trojanowski, J.Q., 1992. The disordered neuronal cytoskeleton in Alzheimer's disease. Curr. Opin. Neurobiol. 2, 653–6.

Liu, Y., Qing, H., Deng, Y., 2014. Biomarkers in Alzheimer's disease analysis by mass spectrometry-based proteomics. Int. J. Mol. Sci. 15, 7865–7882. doi:10.3390/ijms15057865

Loo, F.-C., Ng, S.-P., Wu, C.-M.L., Kong, S.K., 2014. An aptasensor using DNA aptamer and white light common-path SPR spectral interferometry to detect cytochrome-c for anti-cancer drug screening. Sensors Actuators B Chem. 198, 416–423. doi:10.1016/j.snb.2014.03.077

Lu, Q., Wood, J.G., 1993. Functional studies of Alzheimer's disease tau protein. J. Neurosci. 13, 508–15.

Mandelkow, E.M., Mandelkow, E., 1998. Tau in Alzheimer's disease. Trends Cell Biol. 8, 425–7.

Martic, S., Rains, M.K., Kraatz, H.-B., 2013. Probing copper/tau protein interactions electrochemically. Anal. Biochem. 442, 130–7. doi:10.1016/j.ab.2013.07.015

Mattsson, N., Zetterberg, H., Hansson, O., Andreasen, N., Parnetti, L., Jonsson, M., Herukka, S.-K., van der Flier, W.M., Blankenstein, M.A., Ewers, M., Rich, K., Kaiser, E., Verbeek, M., Tsolaki, M., Mulugeta, E., Rosén, E., Aarsland, D., Visser, P.J., Schröder, J., Marcusson, J., de Leon, M., Hampel, H., Scheltens, P., Pirttilä, T., Wallin, A., Jönhagen, M.E., Minthon, L., Winblad, B., Blennow, K., 2009. CSF biomarkers and incipient Alzheimer disease in patients with mild cognitive impairment. JAMA 302, 385–93. doi:10.1001/jama.2009.1064

Mehta, P.D., Pirttilä, T., Mehta, S.P., Sersen, E.A., Aisen, P.S., Wisniewski, H.M., 2000. Plasma and cerebrospinal fluid levels of amyloid beta proteins 1-40 and 1-42 in Alzheimer disease. Arch. Neurol. 57, 100–5.

Murray, M.E., Graff-Radford, N.R., Ross, O.A., Petersen, R.C., Duara, R., Dickson, D.W., 2011. Neuropathologically defined subtypes of Alzheimer's disease with distinct clinical characteristics: a retrospective study. Lancet. Neurol. 10, 785–96. doi:10.1016/S1474-4422(11)70156-9

Perrin, R.J., Fagan, A.M., Holtzman, D.M., 2009. Multimodal techniques for diagnosis and prognosis of Alzheimer's disease. Nature 461, 916–22. doi:10.1038/nature08538

Price, J.L., Morris, J.C., 1999. Tangles and plaques in nondemented aging and "preclinical" Alzheimer's disease. Ann. Neurol. 45, 358–68.

Rains, M.K., Martić, S., Freeman, D., Kraatz, H.B., 2013. Electrochemical investigations into kinase-catalyzed transformations of tau protein. ACS Chem. Neurosci. 4, 1194–203. doi:10.1021/cn400021d

Rushworth, J.V., Ahmed, A., Grif, H.H., Pollock, N.M., Hooper, N.M., Millner, P.A, 2014. Biosensors and Bioelectronics A label-free electrical impedimetric biosensor for the specific detection of Alzheimer's amyloid-beta oligomers 56, 83–90. doi:10.1016/j.bios.2013.12.036

Sharma, R, Deacon, S.E., Nowak. D, George. S.E., Szymonik, M.P., Tang, A.A., Tomlinson, D.C., Davies, A.G., McPherson, M.J., Wälti, C., 2016. Biosensors and Bioelectronics Label-free electrochemical impedance biosensor to detect human interleukin-8 in serum with sub-pg/ml sensitivity 80, 607–613. doi:10.1016/j.bios.2016.02.028

Shoji, M., Matsubara, E., Murakami, T., Manabe, Y., Abe, K., Kanai, M., Ikeda, M., Tomidokoro, Y., Shizuka, M., Watanabe, M., Amari, M., Ishiguro, K., Kawarabayashi, T., Harigaya, Y., Okamoto, K., Nishimura, T., Nakamura, Y., Takeda, M., Urakami, K., Adachi, Y., Nakashima, K., Arai, H., Sasaki, H., Kanemaru, K., Yamanouchi, H., Yoshida, Y., Ichise, K., Tanaka, K., Hamamoto, M., Yamamoto, H., Matsubayashi, T., Yoshida, H., Toji, H., Nakamura, S., Hirai, S.,. Cerebrospinal fluid tau in dementia disorders: a large scale multicenter study by a Japanese study group. Neurobiol. Aging 23, 363–70.

Sparks, D.L., Kryscio, R.J., Sabbagh, M.N., Ziolkowski, C., Lin, Y., Sparks, L.M., Liebsack, C., Johnson-Traver, S., 2012. Tau is reduced in AD plasma and validation of employed ELISA methods. Am. J. Neurodegener. Dis. 1, 99–106.

Sunderland, T., Linker, G., Mirza, N., Putnam, K.T., Friedman, D.L., Kimmel, L.H., Bergeson, J., Manetti, G.J., Zimmermann, M., Tang, B., Bartko, J.J., Cohen, R.M.,. Decreased beta-amyloid1-42 and increased tau levels in cerebrospinal fluid of patients with Alzheimer disease. JAMA 289, 2094–103. doi:10.1001/jama.289.16.2094

Tuantranont, A., 2013. Applications of Nanomaterials in Sensors and Diagnostics.

von Linstow Roloff, E., Platt, B., 1999. Biochemical dysfunction and memory loss: the case of Alzheimer's dementia. Cell. Mol. Life Sci. 55, 601–16.

Wimo, A., Jönsson, L., Bond, J., Prince, M., Winblad, B., 2013. The worldwide economic impact of dementia 2010. Alzheimers. Dement. 9, 1–11.e3. doi:10.1016/j.jalz.2012.11.006

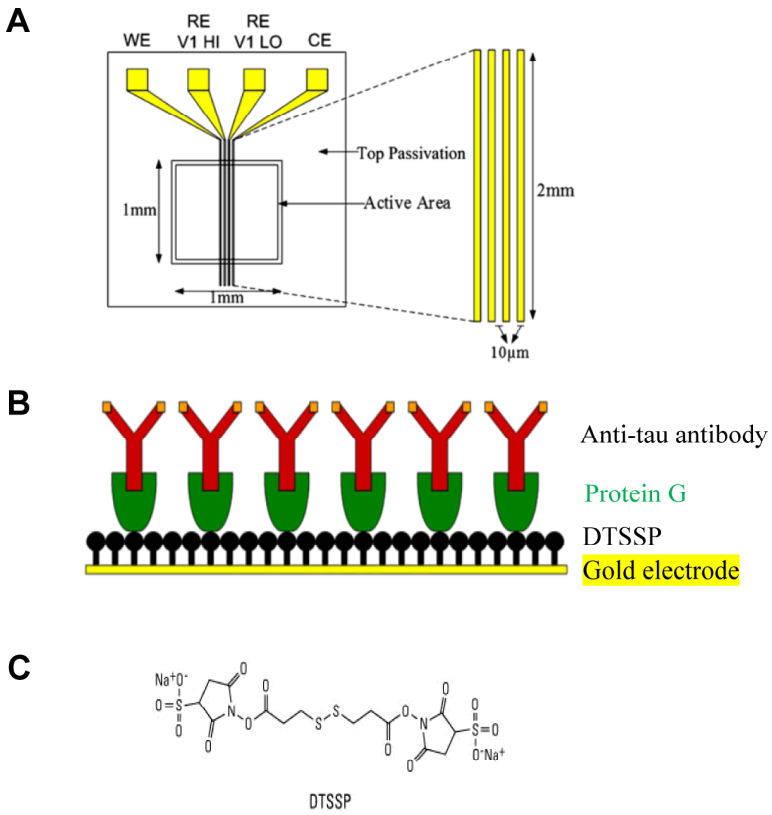

Fig. 1. (A) Details of the purchased gold microband electrodes. It shows the 1 × 1 mm active sensor area and the connections to the impedance analyser. (B) Schematic side view of the biosensor. From bottom to top: gold microband electrode, SAM layer, protein G layer and antibodies. (C) Chemical structure of DTSSP which contains an amine-reactive *N*-hydroxysulfosuccinimide (sulfo-NHS) ester at each end and forms the SAM layer.

Fig. 2. Construction and assembly of the biosensor. (A) Layer-by-layer development of the biosensor verified by EIS. The imaginary component of impedance (Z″) was plotted against the real component of impedance (Z′) in Nyquist plots. Impedance spectra were recorded after each construction stage: (a) bare gold, (b) DTSSP or SAM, (c) protein G, (d) ethanolamine and (e) anti-tau antibody, in 10 mM $K_4Fe(CN)_6/K_3Fe(CN)_6$ (1:1 ratio) in PBS pH 7 over a frequency range of 40-40,000 Hz. Inset shows the Randles′ equivalent circuit model t of the impedance used for fitting where R_s = solution resistance, R_{ct} = charge-transfer resistance and C_p = constant phase element. (B) Interfacial charge-transfer resistance (R_{ct}) variance across the different functionalization steps. (C) Characterization of layer-by-layer construction of the biosensor verified by CV as described in Section 2.2.

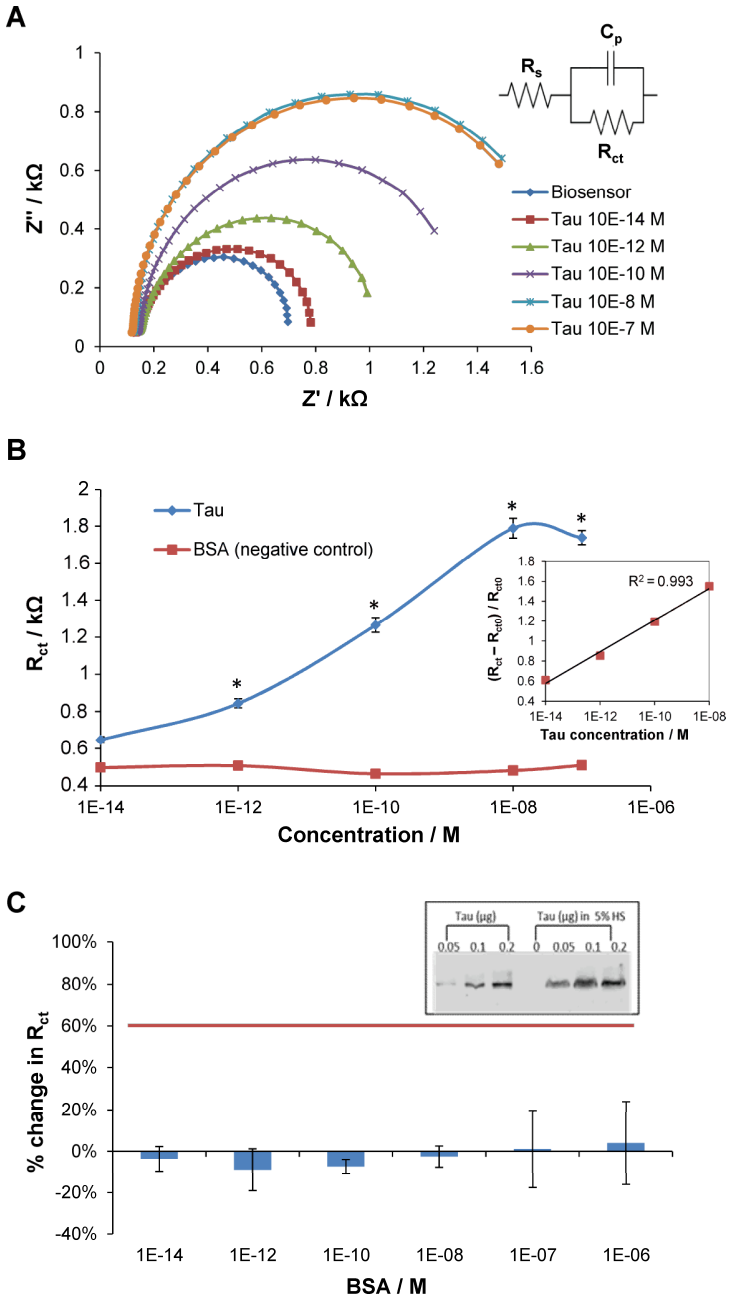

Fig. 3. Biosensor response to increasing tau concentrations measured by EIS. (A) EIS analysis of cumulative incubations with tau (10^{-14} M to 10^{-7} M) in PBS followed by rinsing with dH_2O and PBS in 10 mM $K_4Fe(CN)_6/K_3Fe(CN)_6$ (1:1 ratio) in PBS pH 7 over a frequency range of 40-40,000 Hz. Impedance measurements are presented as Nyquist plots with the imaginary component of impedance (Z″) plotted against the real component of impedance (Z′). Inset shows impedance spectra fitted into a Randles′ equivalent circuit model where R_s = solution resistance, R_{ct} = charge-transfer resistance and C_p = constant phase element. (B) Calibration curves of tau binding to the biosensor. The charge-transfer resistance (R_{ct}) values of the anti-tau antibody interfaces following incubation with tau or BSA were determined by fitting the data to the Randles′ circuit model using Zview software. R_{ct} values for tau and BSA were compared using a two tails t-test assuming unequal variances, *$p < 0.05$. Inset figure shows percentage of R_{ct} change of equilibrated biosensor (R_{ct0}) after incubation with increasing tau concentrations. (C) Influence of increasing BSA concentrations on biosensor response in PBS containing 10 mM $K_4Fe(CN)_6/K_3Fe(CN)_6$ (1:1 ratio) pH 7. A change of < 4% in R_{ct} was seen at 10^{-6} M BSA compared to more than 60% change at 10^{-14} M tau. The horizontal line shows the response to 10^{-14} M tau. Inset figure showed detection of 0.05 to 0.2 µg of tau in PBS or in 5% HS by anti-tau antibody by Western blotting.

Fig. 4. Biosensor response to (A) tau spiked in HS, and (B) HS in a range of dilutions 1:1 to 1:1000 as measured by EIS. EIS analysis of biosensor of incubations with tau (10^{-14} M to 10^{-7} M) in HS followed by rinsing with dH_2O and PBS, in 10 mM $K_4Fe(CN)_6/K_3Fe(CN)_6$ (1:1 ratio) in PBS pH 7 over a frequency range of 40-40,000 Hz. Impedance measurements were presented as Nyquist plots where the imaginary component of impedance (Z″) was plotted against the real component of impedance (Z′). (C) Calibration curves of tau in a dilution of 1:1 HS binding to the biosensor. The % R_{ct} change versus full biosensor (R_{ct0}) after incubation with different tau concentrations in HS were presented as the mean of at least three independent experiments ± SD. The charge-transfer resistance (R_{ct}) values of the anti-tau antibody interfaces following incubation with tau were determined by fitting the data to the Randles′ circuit model using Zview software. These R_{ct} values were compared statistically for tau and HS only using two tailed t-test assuming unequal variances, *$p < 0.05$, **$p < 0.005$, ***$p < 0.001$. The horizontal red line shows the biosensor response to HS only.

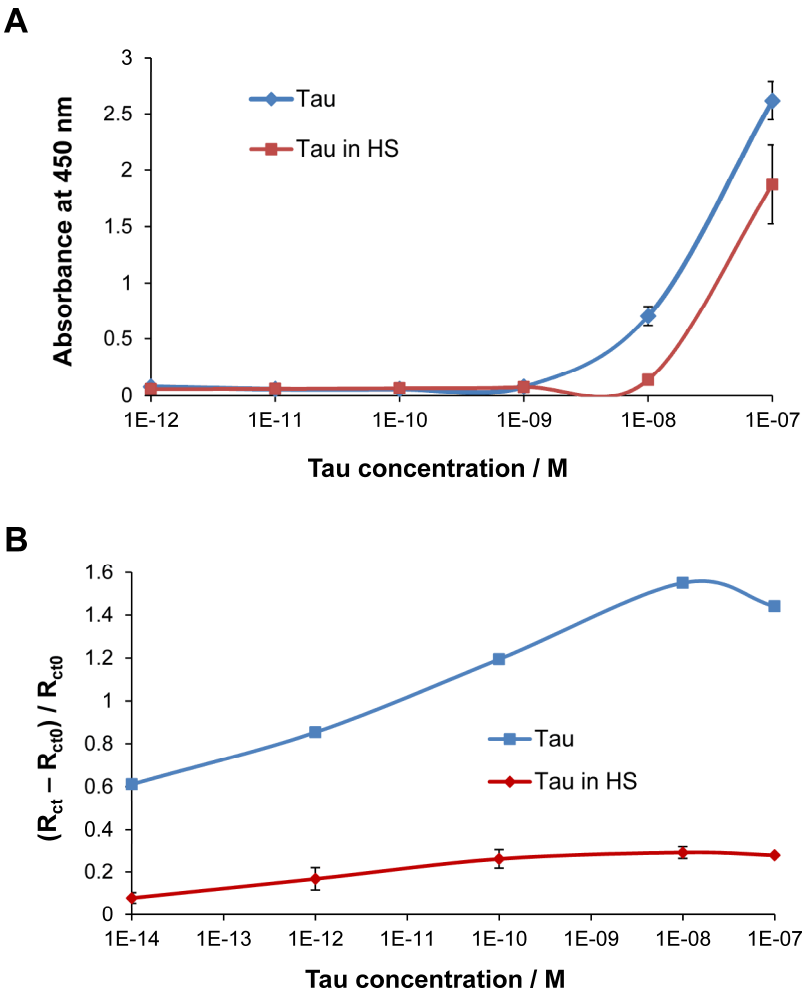

Assay method	LOD (M)	Assay range (M)
Biosensor	10^{-14}	10^{-14} ~ 10^{-7}
ELISA	10^{-8}	10^{-12} ~ 10^{-7}

Fig. 5. Comparison of LOD of tau by ELISA and electrochemical biosensor methods. LOD from biosensor was six orders of magnitude lower than for ELISA. (A) ELISA results showing detection of different tau concentrations (10^{-12} M to 10^{-7} M) in PBS or in 5% HS. (B) Biosensor results showing detection of 10^{-14} M to 10^{-7} M tau in PBS and HS.

Table1.
EIS parameters obtained from fitting the Nyquist plots shown in Fig. 3A to the Randles′ circuit model. The data is presented with standard error.

Electrode	**R_s (Ω)**	**C_p (nF)**	**R_{ct} (Ω)**
Biosensor	130.6±1.9	159.7±2.9	592.3±14.3
Tau 10^{-14} M	139.2±2.0	159.7±2.8	647.1±16.9
Tau 10^{-12} M	150.0±2.2	156.6±2.6	844.1±24.5
Tau 10^{-10} M	142.8±2.0	154.6±2.0	1266.0±39.4
Tau 10^{-8} M	125.6±1.5	128.5±1.3	1789.0±53.0
Tau 10^{-7} M	119.0±1.1	123.5±9.3	1739.0±37.8